# OPTIMUM DESIGN OF MICRO THERMAL FLOW SENSOR AND ITS EVALUATION IN WALL SHEAR STRESS MEASUREMENT

Takashi Yoshino[1], Yuji Suzuki[1], Nobuhide Kasagi[1] and Shoji Kamiunten[2]
[1]Department of Mechanical Engineering, The University of Tokyo
7-3-1 Hongo, Bunkyo-ku, Tokyo 113-8656, Japan
Tel: +81-3-5841-6419 Fax: +81-3-5800-6999 E-mail: yoshino@thtlab.t.u-tokyo.ac.jp
[2]Yamatake Corporation, 1-12-2 Kawana, Fujisawa, Kanagawa 251-8522, Japan

## ABSTRACT

A numerical analysis of unsteady conjugate heat transfer for micro thermal flow sensor was made in order to improve its frequency response in the wall shear stress measurement. It is found that there exists a limit of the frequency response even for the ideal sensor that has no heat conduction loss to the substrate. Heat conduction in the fluid and indirect convective heat transfer from the diaphragm are two major mechanism of deteriorating the sensor response. We propose an optimum arrangement of the hot-film and diaphragm based on the detailed numerical simulation of the thermal field, and evaluate its performance in turbulent flow measurements.

## INTRODUCTION

Up to now, various kinds of micro thermal sensors were proposed for flow measurement [1]. It is believed that thermal insulation of the heater element from the substrate is crucial in order to increase the frequency response [2]. For instance, Liu et al.[3] made an insulating vacuum cavity underneath thin diaphragm having 200×200μm$^2$ for their hot-film shear stress sensor. They applied sinusoidal electrical signal to the constant temperature circuit and estimated the cutoff frequency to be 9kHz. However, since such electrical test is not equivalent to real measurement condition, direct evaluation of the sensor response in unsteady flows should also be made. The objectives of the present study are to elucidate thermal field around micro thermal flow sensor using unsteady numerical simulation and to propose optimum arrangement of the hot-film and diaphragm. Moreover, micro hot-film wall shear stress sensor was fabricated based on the present numelical analysis, and its performance was evaluated in turbulent channel flow, where power spectra of the fluctuations is well described.

## FABRICATION PROCESS

Figure 1 shows the simplified process flow of the wall shear stress sensor. First, silicon nitride ($SiN_x$) is deposited on both sides of a 0.3mm thick (100) silicon wafer. An 0.1μm-thick platinum (Pt) is then deposited on the front side and patterned by photolithography and dry etching to provide a heater and an ambient temperature sensor. Another layer of $SiN_x$ is deposited, and the platinum patterns are encapsulated by the totally about 1μm thick $SiN_x$. This is followed by dry etching of $SiN_x$ diaphragm for the thermal isolation slits on the both sides of the Pt heater. On the backside of the wafer, the $SiN_x$ layer is patterned into a square opening. In order to release the diaphragm structure, the bulk of the silicon is removed by anisotropic wet etching, and an air cavity that consists of four (111) plane of the silicon wafer is fabricated. In our previous studies [4], we used anisotropic etch from the front side through etch hole to make the air cavity. In the present fabrication process, we employ etch from the backside in order to make more flexible design of the diaphragm possible and realize the optimum diaphragm arrangements described later.

## NUMERICAL ANALYSIS

Figure 2 shows our first-generation hot-film sensor (Type 1) having a platinum heater on 1 μm-thick $SiN_x$ diaphragm [4]. In order to keep sufficiently large electric resistance of the hot-film, a thin line of platinum is patterned zigzag in an area of 300×32μm$^2$. A deep air cavity having 200μm in depth is wet-etched into the Si substrate through slits on the diaphragm. We evaluated the response of Type 1 sensor in a turbulent channel

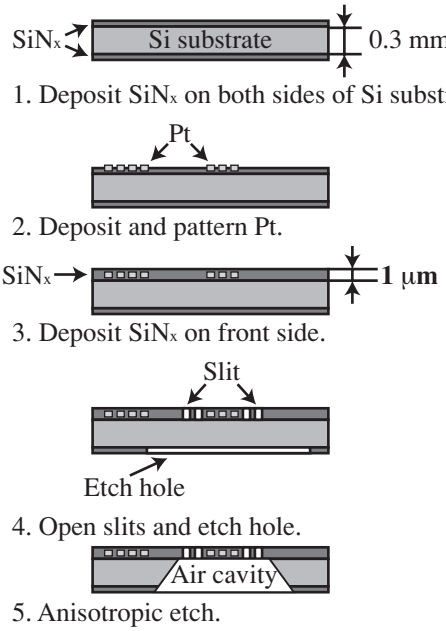


Fig. 1 Process flow of micro wall shear stress sensor..

flow, and found that the frequency response is surprisingly low; the gain is flat only below 70Hz [4]. This fact motivated us to employ numerical simulation to examine the thermal field around hot-film in detail.

Figure 3 shows the two-dimensional computational model used in the present study. In order to mimic the fluctuating flow velocity near the wall, the fluid velocity was given as a linear function of the distance to the wall, and the amplitude of the fluctuation is set to be 40% of the mean wall shear stress. Since the velocity profile is given, the governing equation for the thermal field is,

$$\frac{\partial T^*}{\partial t^+} + u^+ \frac{\partial T^*}{\partial x^+} = \frac{1}{\mathrm{Pr}}\left(\frac{\partial^2 T^*}{\partial x^{+2}} + \frac{\partial^2 T^*}{\partial y^{+2}}\right), \qquad (1)$$

where $x^+$ and $y^+$ denote nondimensionalized distance using the mean velocity gradient at the wall $dU/dy$ and the kinematic viscosity ν. Fluid is assumed to be air and the Prandtl number Pr (=ν/α) is set to be 0.7. The velocity gradient $dU/dy$ is 11000s$^{-1}$, which corresponds to the experimental condition in a turbulent channel flow described later. The thermal conductivity of $SiN_x$ is assumed to be 23.4W/(m·K), although thermal property of $SiN_x$ depends on its deposition process. Constant temperature circuit with ideal response is assumed, and the temperature of the hot-film is kept constant in the present simulation.

Figure 4 shows the frequency response of 'ideal' sensor with adiabatic wall. Although there exists no heat conduction loss to the substrate for this sensor, the gain is decreased with increasing frequency. Note that the horizontal axis is scaled with so-called viscous scale $f^+(=fdU/dy)$, and the response of sensors having different hot-film length in the streamwise direction almost

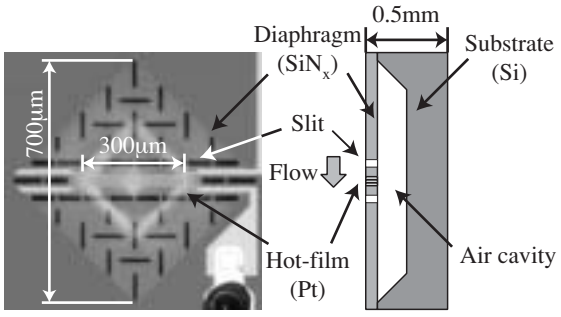


Fig. 2 Magnified view of micro hot-film shear stress sensor (Type 1)[4] .

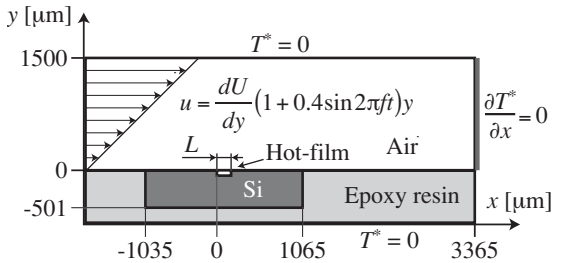


Fig. 3 Computational domain and boundary condition.

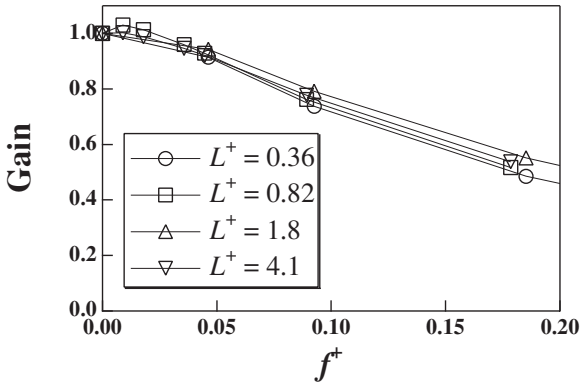


Fig. 4 Frequency response of sensor model with adiabatic wall.

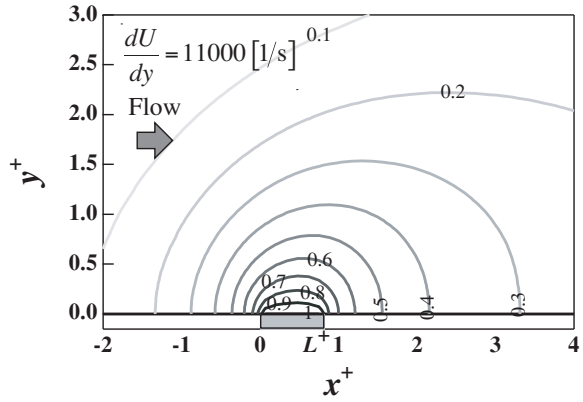


Fig. 5 Temperature distribution around the sensor model with adiabatic wall.

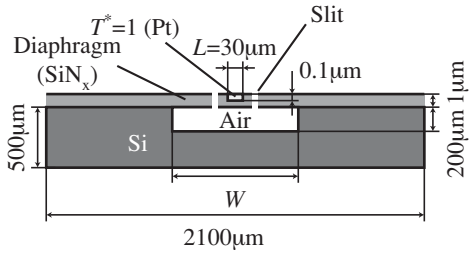


Fig. 6 Schematic of sensor model (not to scale).

collapses to a single curve. Therefore, once $dU/dy$ is given, an upper limit of the frequency response of the thermal wall shear stress sensor having continuous surface is determined, no matter how the heat conduction to the substrate is suppressed. This is because the temperature distribution spreads out to the upstream and downstream directions due to the heat conduction in fluid, and this 'thermal cloud' inhibits the hot-film to be exposed to the ambient temperature (Fig. 5).

We numerically examined the response of the sensor models having thermal insulation slit on the both sides of the hot-film (Fig. 6). The length of $SiN_x$ diaphragm was chosen as $W$=700μm, which corresponds to Type 1 (Fig. 2), 200μm, and 300μm. Figure 7 shows variation of the wall shear stress determined with the sensor model $\tau_{w,meas.}$ versus true wall shear stress $\tau_{w,true}$ during one oscillation cycle. Because of the imperfect

frequency response of the sensor, $\tau_{w,meas.}$ for $W$=700μm has relatively large phase lag over $\tau_{w,true}$, and the gain is decreased with increasing frequency. On the other hand, for $W$=200μm, the gain and phase lag are much improved.

Figure 8 shows the gain for various sensor models. Frequency response is increased with decreasing diaphragm- length $W$. The frequency response for $W$=200~300μm is higher than the sensor model with adiabatic wall described above. This is because thermal conductivity of air is three orders of magnitude smaller than that of $SiN_x$, and the slits inhibit tangential heat conduction in the diaphragm. As shown in Fig. 9a, the extent of 'thermal cloud' is confined between the slits, and contours of the temperature field becomes

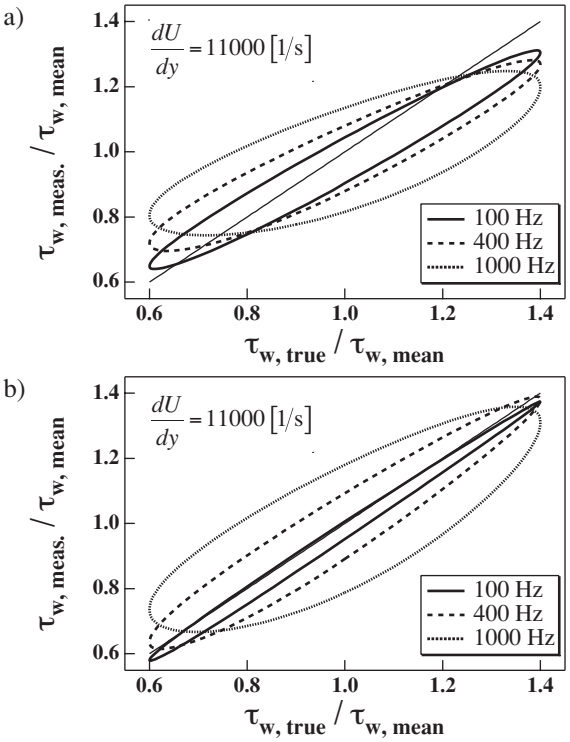


Fig. 7 Wall shear stress fluctuation determined with sensor models during one oscillation cycle. a) $W$=700 μm, b) $W$=200 μm.

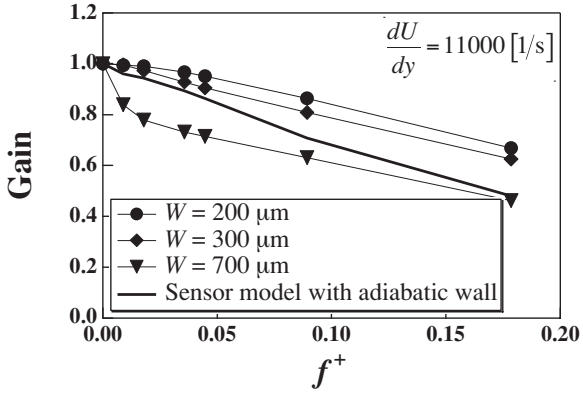


Fig. 8 Frequency response of the sensor models.

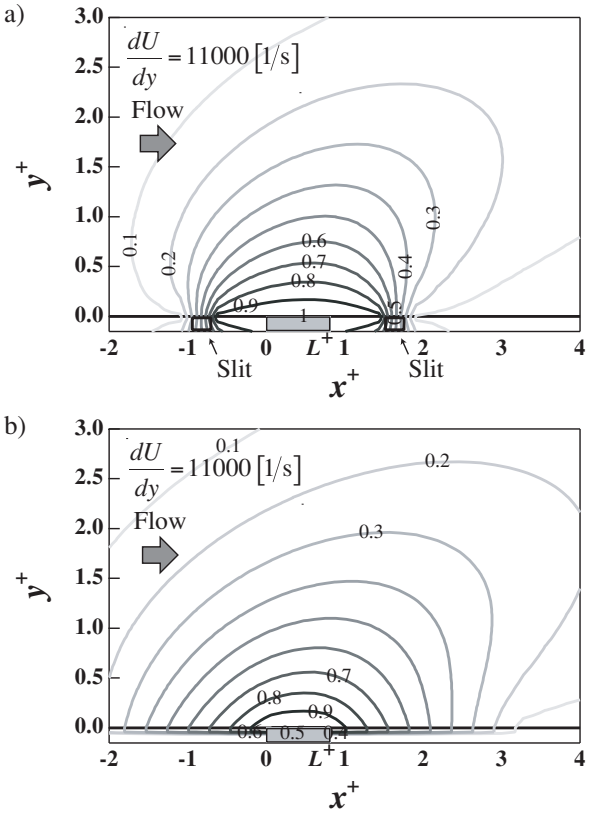


Fig. 9 Temperature distribution around the sensor model. a) $W$=200μm, b) vacuum cavity, $W$=200μm.

dense especially close to the slits. Figure 9b shows temperature distribution of the sensor model assuming a vacuum cavity underneath the diaphragm, which is used by Liu et al. [3]. The temperature distribution exhibits a similar trend as in Fig. 5. Therefore, sensors with air cavity and slits on the diaphragm should have superior response than sensors with continuous diaphragm and vacuum cavity underneath.

When the overheat temperature is 60K, the total heat consumption per unit spanwise length for the sensor models is respectively 5.7 W/m, 6.8 W/m, and 29.5 W/m for $W$=700μm, $W$=200μm, and the vacuum cavity sensor. Therefore, sensors with air slits have an advantage also in terms of the energy consumption. Since the cavity is sufficiently deep in the present sensor models, heat conduction loss through the cavity is minor. Note that the energy consumption is increased when the diaphragm length is further reduced. Therefore, $W$=200-300μm should be the optimum length in the present flow condition.

## EXPERIMENTAL EVALUATION

Figure 10 shows our second-generation sensor (Type 2) based on our numerical results. The length of the diaphragm was chosen as 200μm. Turbulent channel flow facility having a channel width of 50mm was employed for the measurement. The bulk mean velocity is

2.5-9.3 m/s. Figure 11 shows the power spectrum of the wall shear stress fluctuation. The frequency response of Type 2 is markedly improved over that of Type 1, and its power spectrum is in good agreement with the most reliable numerical simulation data [5] up to $f^+$=0.02. This trend is in good agreement with the simulation result shown in Fig. 8. On the other hand, response of Type 1 is much worse than the numerical prediction. It is conjectured that this is due to the fact that the distance between the hot-film and the slits on the diaphragm of Type 1 is 2.5 times larger than that of Type 2. Figure 12 shows the root-mean-square vale of the streamwise wall shear stress fluctuation $\tau_{w\ rms}$ normalized by its mean value $\tau_{w\ mean}$. Again, measurement data by Type 2 are in good agreement with the DNS data [5], [6] at

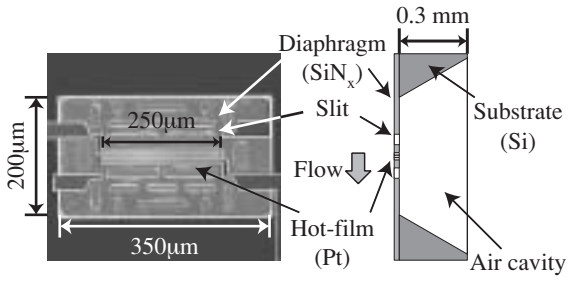


Fig. 10 Magnified view of micro hot-film shear stress sensor presently developed (Type 2).

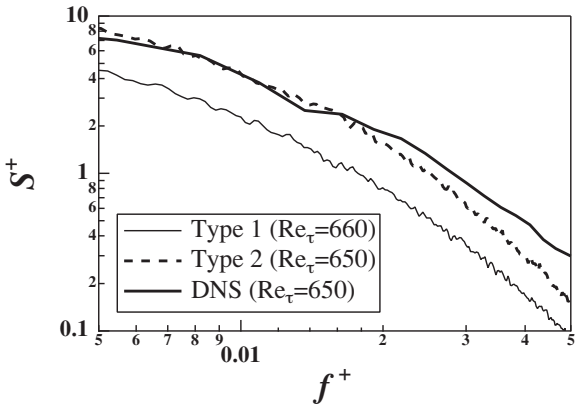


Fig. 11 Power spectrum of wall shear stress fluctuations in turbulent channel flow and their comparison with the DNS result [5].

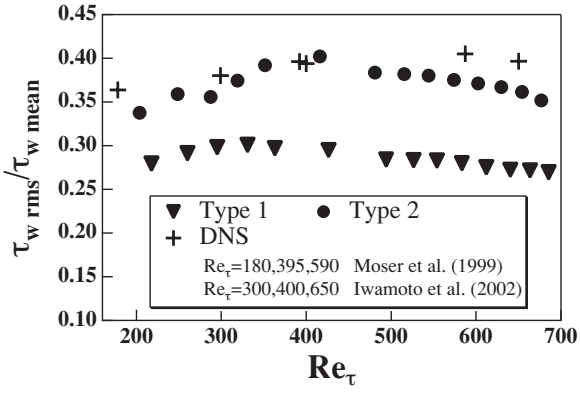


Fig. 12 Rms values of wall shear stress fluctuations.

the Reynolds number $Re_\tau$<400, and slightly decreased with increasing $Re_\tau$.

## CONCLUSIONS

Detailed numerical simulation of the thermal field around micro hot-film wall shear stress sensor was made. It is found that heat conduction to the fluid has large effect on the sensor response, and there exists an upper limit of the frequency response, even if the heat conduction loss to the substrate is negligible. The sensor models having deep air cavity exhibit better performance than vacuum cavity sensor, if the diaphragm length is carefully chosen. Based on the present numerical results, we propose an optimal design of micro hot-film shear stress sensor and evaluate its performance in a physical experiment. The response of the present sensor is markedly improved over our previous sensor.

## ACKNOWLEDGMENTS

The authors are grateful to Messrs. N. Zushi, S. Nakano, and T. Nakata in Yamatake Corp. for their corporation in manufacturing micro thermal sensor. This work was supported through the Project for Organized Research Combination System by the Ministry of Education, Culture, Sports, Science and Technology of Japan (MEXT).

## REFERENCES

[1] A. Rasmussen, and M. E. Zaghloul, "In the flow with MEMS," *IEEE Circuits & Devices*, Vol. 14, No. 4, 1998, pp. 12-25.

[2] P. H. Alfredsson, A. V. Johansson, J. H. Haritonidis, and H. Eckelmann, "The fluctuating wall-shear stress and the velocity field in the viscous sublayer," *Phys. Fluids*, Vol. 31, No. 5, 1988, pp. 1026-1033.

[3] C. Liu, J.-B. Huang, Z. A. Zhu, F. Jiang, S. Tung, Y.-C. Tai, and C.-M. Ho, "A micromachined flow shear-stress sensor based on thermal transfer principles," *J. Microelectromech. Syst.*, Vol. 8, No. 1, 1999, pp. 90-99.

[4] T. Yoshino, Y. Suzuki, N. Kasagi, and S. Kamiunten, "Assessment of the wall shear stress measurement with arrayed micro hot-film sensors in a turbulent channel flow," *Proc. 2nd Int. Symp. Turbulence and Shear Flow Phenomena*, Vol. 2, Stockholm, Sweden, 2001, pp. 153-158.

[5] K. Iwamoto, Y. Suzuki, and N. Kasagi, "Reynolds number effect on wall turbulence: toward effective feedback control," *Int. J. Heat Fluid Flow*, Vol. 23, No. 5, 2002, pp. 678-689.

[6] R. D. Moser, J. Kim, and N. N. Mansour, "Direct numerical simulation of turbulent channel flow up to $Re_\tau$=590," *Phys. Fluids*, Vol. 11, No. 4, 1999, pp. 943-945.